

HST FOS OBSERVATIONS OF YY DRA

CAROLE A. HASWELL, JOSEPH PATTERSON

Columbia University, 538 W. 120th St., NY, NY 10027, USA

Abstract. The UV continuum of YY Dra exhibits a sinusoidal modulation with 15.5% semi-amplitude and period 264.7 s, commensurate with one half the white dwarf spin period. The C IV line profile varies with spin phase, implying accretion onto, and visibility of, both magnetic poles. The line width is greatest at the phases of continuum pulsation maximum, when the wings extend out to $\pm 3000 \text{ km s}^{-1}$. This implies a minimum white dwarf mass of $0.62 M_{\odot}$, and constrains the angle between the line of sight and the magnetic axis.

1. Introduction

Coherent X-ray pulsations (Beuermann & Thomas 1993; Patterson & Szkody 1993) have confirmed YY Dra as a DQ Her star/intermediate polar (Patterson et al. 1992; Patterson 1994; Hellier 1996). The X-ray and optical data imply a white dwarf spin period, P_{spin} , of 529 s, and variable accretion geometry: sometimes modulation occurs predominantly at P_{spin} , while at other times $P_{\text{spin}}/2$ dominates.

We present a brief discussion of high time resolution UV observations of YY Dra¹; a full presentation will be given in Haswell et al. (1996).

2. Observations

HST observed YY Dra on 1994 June 8...9. FOS/RAPID mode with the G130 grating was used, yielding a time resolution of 5.6 s, a duty cycle of 87%, and coverage of 1147...1605 Å. The spectrum reveals strong C IV $\lambda\lambda 1548.1, 1550.8$ emission and several other line emission features.

¹Based on observations with the NASA/ESA Hubble Space Telescope obtained at the Space Telescope Science Institute, which is operated by the Association of Universities for Research in Astronomy, Incorporated, under NASA contract NAS5-26555

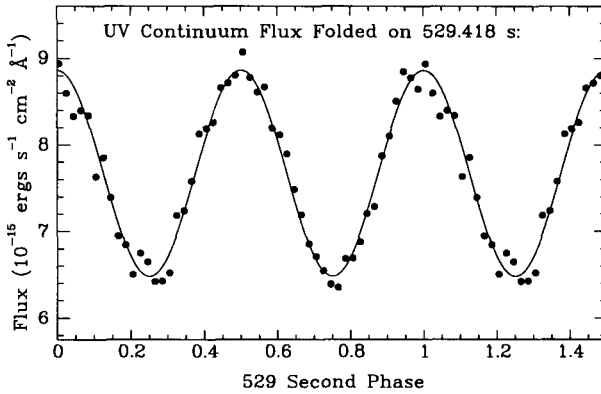


Figure 1. The UV continuum light folded on the inferred white dwarf spin period, 529.4 s; the modulation occurs purely at one half the spin period: 264.7 s.

2.1. THE UV CONTINUUM PULSATIONS

A UV continuum light curve was generated by computing the mean flux in the region 1420...1525 Å for each of the 3873 individual exposures. Strong pulsations were detected. The best-fitting sine wave has period 264.709 ± 0.05 s, with mean flux $7.67 \times 10^{-15} \text{ erg s}^{-1} \text{ cm}^{-2} \text{ Å}^{-1}$ and a semi-amplitude of 15.5%. Fig. 1 shows the light curve folded on a period of 529.418 s: there are no significant deviations from a sinusoidal modulation with period 264.7 s. If the emission is due to two-pole accretion with $P_{\text{spin}} = 529.4$ s, then we must conclude that the accretion geometry produced extremely symmetric pulses at the epoch of our HST observations.

2.2. PULSATIONS IN THE UV LINES

To search for line profile modulations, our spectra were folded on the inferred spin period: 529.4 s. Fig. 2 shows the trailed spectrogram of the CIV line after subtracting the (spin-phase dependent) continuum. The line profile variations are subtle, but the line centre flux is weakly pulsed (4.4% semi-amplitude) in antiphase with the underlying continuum pulsations, and broad wings appear at the phases of continuum maxima. These wings appear simultaneously on both sides of the line and extend out to $\pm \sim 3000 \text{ km s}^{-1}$.

3. Discussion and conclusions

The most plausible origin for the high velocity emission is radially infalling material in the accretion columns. Assuming free-fall from infinity, a radial velocity of 3000 km s^{-1} is attained at $r = 2.5 \times 10^9 \cos^2(|\alpha - i|) \text{ cm}$; here

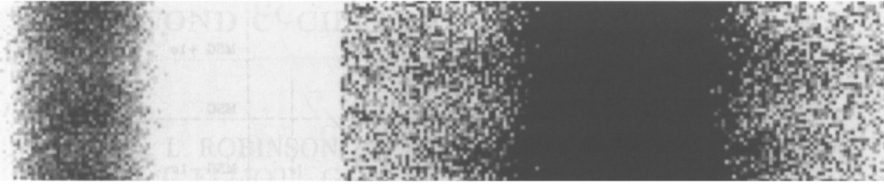


Figure 2. The trailed spectrogram of the CIV line emission after folding the data on the white dwarf spin period. The same data appear twice: on the left-hand side with grayscale adjusted to show the line center modulations; on the right-hand side to show the modulations in the wings. Spin phase increases (through one 529-s cycle) vertically upwards, and wavelength increases to the right.

α is the angle between the magnetic axis and the spin axis of the white dwarf, i is the orbital inclination, and a white dwarf mass of $M_{\text{wd}} = 0.85 M_{\odot}$ has been used (Mateo, Szkody & Garnavich 1991, henceforth MSG). This corresponds to about four white dwarf radii (r_{wd}) from the center of the white dwarf. Since we see both red *and* blue wings, we are seeing two columns simultaneously. Hence, we can definitely rule out the hypothesis of there being only one accreting column from which the radiation beaming pattern produces two flux maxima per white dwarf spin period. Maximum radial velocity occurs when the accretion columns are most closely aligned with our line of sight. Thus we deduce that the maximum continuum flux also occurs when the accretion columns are aligned with our line of sight.

For infalling material in the far column with radial velocity K to be visible, rather than being occulted by the white dwarf, we require:

$$\sin(|\alpha - i|) \cos^2(|\alpha - i|) \geq \frac{r_{\text{wd}} K^2}{2GM_{\text{wd}}}. \quad (1)$$

The Hamada-Salpeter mass-radius relation: $r_{\text{wd}} \approx 0.56(M_{\text{wd}}/0.85 M_{\odot})^{-0.8}$ then gives a minimum allowed value of M_{wd} for any $|\alpha - i|$. This relationship for $K = 3000 \text{ km s}^{-1}$ is the curve shown in Fig. 3; the region of parameter space below the curve is disallowed. Hence the CIV line profile implies a minimum white dwarf mass of $0.62 M_{\odot}$. This is in good agreement with the completely independent mass determination of MSG.

MSG also determined the orbital inclination of the system: $i = 42^{\circ} \pm 5^{\circ}$. Since both α and i are $< 90^{\circ}$, this implies $|\alpha - i| < 53^{\circ}$; which yields the vertical dotted line in Fig. 3. Putting all these constraints together requires the parameters to lie within the region bounded by the MSG $\pm 1\sigma$ mass limits at the top and bottom; on the left by our curve, and on the right

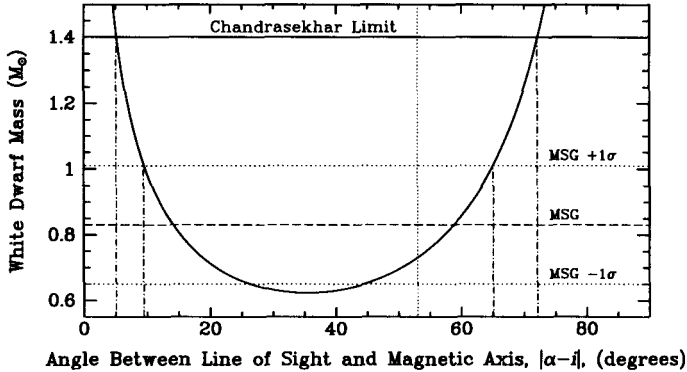


Figure 3. Constraints on white dwarf mass: the region of parameter space below the curve is disallowed (see text). Hence a minimum white dwarf mass of $0.62 M_{\odot}$ is derived. MSG's independent mass determination (lower three horizontal lines) agrees well. The Chandrasekhar upper limit on the white dwarf mass leads to the outer pair of dot-dashed vertical lines delimiting the allowed angle. The inner pair of dot-dashed vertical lines delimit the allowed range of angles arising from the combination of the MSG mass and the curve resulting from the C IV line width. The dotted vertical line at 53° is the constraint which arises from MSG's orbital inclination: the region to the right of this line is disallowed.

by our curve and $|\alpha - i| < 53^{\circ}$. We can add a further weak qualitative constraint by noting (Fig. 1 and Fig. 2) that the two accretion columns appear remarkably similar to us. This is easiest to understand if $\alpha \sim 90^{\circ}$, and $|\alpha - i|$ is towards the right hand side of the allowed region. A similar requirement on the orientation of the magnetic axis in DQ Her was recently argued by Robinson et al. (1996) and Zhang et al. (1996).

Acknowledgments. Support for this work was provided by NASA through grant number GO-5500-01-93A from the Space Telescope Science Institute, which is operated by the Association of Universities for Research in Astronomy, Incorporated, under NASA contract NAS5-26555.

References

- Beuermann, K., Thomas, H.-C., 1993, *Adv. Space Res.*, **13**(12), 115
 Haswell, C.A., Patterson, J., Hellier, C., et al., 1996, in preparation.
 Hellier, C., 1996, these proceedings, p143
 Mateo, M., Szkody, P., Garnavich, P., 1991, *Ap. J.*, **370**, 370
 Patterson, J., 1994, *PASP*, **106**, 209
 Patterson, J., Schwartz, D.A., Pye, J.P., et al. 1992, *Ap. J.*, **392**, 233
 Patterson, J., Szkody, P., 1993, *PASP*, **105**, 1116
 Robinson, E.L., Zhang, E., Bless, R.C., et al., 1996, these proceedings, p173
 Zhang, E., Robinson, E.L., Stiening, R.F., Horne, K., 1996, *Ap. J.*, in press